Submitted to the Australasian Tunnelling Society (ATS)

The David Sugden Young Engineers Award for 2009

BACK-ANALYSIS BASED ON THE PINHEIROS STATION COLLAPSE

By David A.F. Oliveira

Number of words: **4491 (including abstract, acknowledgements and references)**
Number of tables: **03**
Number of figures: **10**

BACK-ANALYSIS BASED ON THE PINHEIROS STATION COLLAPSE

David A. F. Oliveira[1]
School of Civil, Mining and Environmental Engineering, University of Wollongong, Australia

ABSTRACT

The Pinheiros Station incident occurred on 12 January 2007, during bench excavation of one of its platform tunnels. The station is located in a dense urban area of the largest city of Brazil, Sao Paulo, and its collapse caused enormous material damages with seven fatalities. The Institute for Technological Research of Sao Paulo (IPT) was appointed by the State Government to undertake one of the most comprehensive forensic investigations in the Brazilian Engineering history. In the final report, IPT stated that an over-simplified geomechanical model was assumed in the design disregarding geological structures, whereby the likely formation of wedges in the roof and side walls of the station cavern which could have significantly contributed to the kinematics of the collapse. In this study a numerical back-analysis based on the station excavation is presented and a possible kinematics of the collapse discussed. In addition, the effect of clay-infilled discontinuities is investigated and two different joint models are compared. The numerical model seems to describe the tunnel behaviour during excavation with acceptable agreement.

1 INTRODUCTION

The Yellow Line of the São Paulo (Brazil) Metro is 12.5 km long and links the city centre to the western suburbs with four interchange stations. The stations are under construction by either cut and cover or NATM methods. The Pinheiros Station was being built by sequential excavation method (NATM) and included a large-diameter shaft (40 m diameter x 36 m in depth), two platform tunnels (18.6 m wide x 14.2 m high x 46 m long) and two access tunnels. The station has side-platforms with a central double-track tunnel (9.6 m diameter). The components of the Pinheiros Station are depicted in Fig. 1.

The Pinheiros Station incident occurred on 12 January 2007, during bench excavation of one of its platform tunnels. The bench excavation started from the running tunnel end towards the shaft. The collapse took place when the bench excavation was almost complete, i.e. close to shaft. The collapse day-lighted in the form of a large crater at Capri Street (Fig. 2). Further details about the construction and the accident are presented by Barros *et al.* (2008).

[1] PhD candidate, Faculty of Engineering, University of Wollongong, NSW 2522, Australia.
Email: dafo407@gmail.com

Paper submitted to the Australasian Tunnelling Society (ATS) for the 2009 David Sugden Young Engineers Award

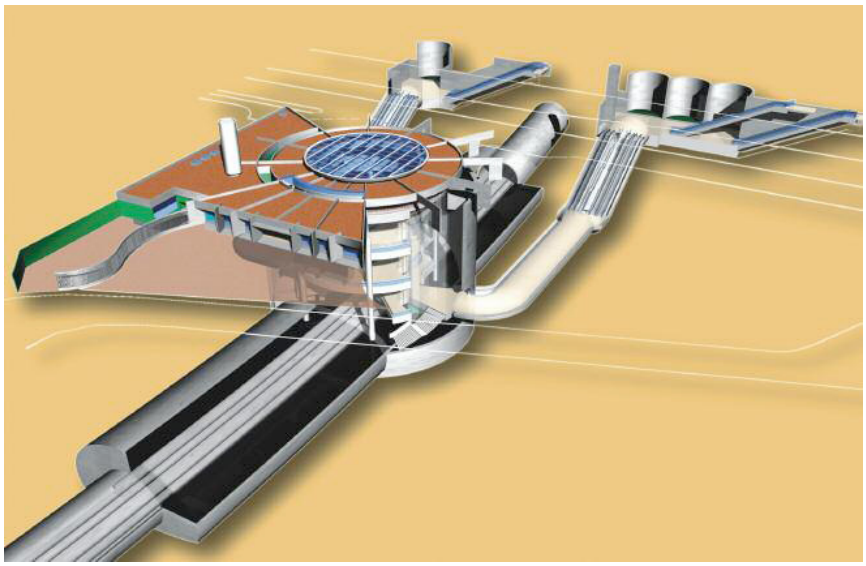

Fig. 1. Artist's impression of the Pinheiros Station (after Barros *et al.* 2008).

Fig. 2. São Paulo Metro station collapse (photo courtesy of Ayrton Vignola/ Folha de S.Paulo).

The Institute for Technological Research of Sao Paulo (IPT) was officially appointed by the State Government to investigate the causes of the collapse. The investigation conducted by IPT involved the analysis of all documentation that could potentially be related to the accident, from the bidding process to final design and construction reports and drawings, including data and follow-up reports of the works. In addition, a thorough archaeological excavation of the collapse debris was carried out, including: geological mapping of the collapse area and residual structures; mapping and photography of the debris, determining its geographical position, as well as material testing.

In the final report, IPT (2008) stated that an over-simplified geomechanical model was assumed in the design disregarding geological structures, whereby the likely formation of wedges in the roof and side walls of the station cavern which could have significantly contributed to the kinematics of the collapse. Based on such an over-simplified model, the proposed open support system (heading arch and footings) could have been inadequate resulting in failure zones under the arch footings (bench side walls). Moreover, the role of sediment infilled joints that were observed during excavation had not been taken into account. Similar assessments were also reported by other investigators (Barton, 2008; Maffei *et al*., 2008).

In this scenario, which involves the inherent complex nature of the cavern excavated by a sequential method (i.e. NATM), a numerical back-analysis is a valuable tool for a better understanding of the collapse kinematics. The numerical procedure may be configured in such a way that the results of field measurements and data from the forensic investigation can be used as input data to determine some of the controlling parameters to completely describe the analysis model in concern. Therefore, in order to investigate the possible mechanism discussed above, Indraratna *et al*. (2009b) presented a 3D numerical simulation of the station excavation, including the effects of a large rock wedge formed in the cavern roof which is structurally controlled by clay-infilled joints.

2 MODELLING PROCEDURE AND ASSUMPTIONS

In order to investigate a possible kinematics of the collapse, a 3D analysis was carried out by Indraratna *et al*. (2009b) using the numerical code FLAC3D. The model includes: all station components (i.e. shaft and platform tunnel, and running tunnel); excavation and support installation sequences as built; full support system (i.e. shotcrete lining, lattice girders and forepoling) as depicted in Fig. 3; and a large rock wedge in the roof of the platform tunnel that is structurally controlled by soil-infilled discontinuities. Only one quarter of the problem is modelled, assuming symmetry planes (Fig. 4).

The typical cross-section of the platform tunnel included a sprayed concrete arch for the heading (350 mm thick, enlarged to 580 mm at the base to conform the footing of the top heading, known as “elephant feet”), reinforced with lattice girders spaced at 830mm, and lateral walls of sprayed concrete for the bench (150 mm thick) reinforced with steel fibres. The invert had only a thin layer (70 mm) of sprayed concrete, with no structural function. If necessary, steel bolts could be applied during bench excavation. Five sets of 12 m long steel forepoles were designed but only three sets were used as a pre-support measure. The construction sequence was (i) excavation of the shaft down to the first working level (invert of the platform top headings); (ii) simultaneous excavation of the headings of the two platform tunnels in opposite directions; (iii) excavation of the bench (second working level) and then, (iv) the excavation of the invert of the platform tunnels. During excavation of the platform tunnels, the top heading advanced in steps of 1.60 m from the shaft towards the running tunnel. The

bench was excavated in advances of 2.0 m from the running tunnel towards the shaft. As mentioned earlier, the invert was not excavated due to the collapse at the end of the bench excavation.

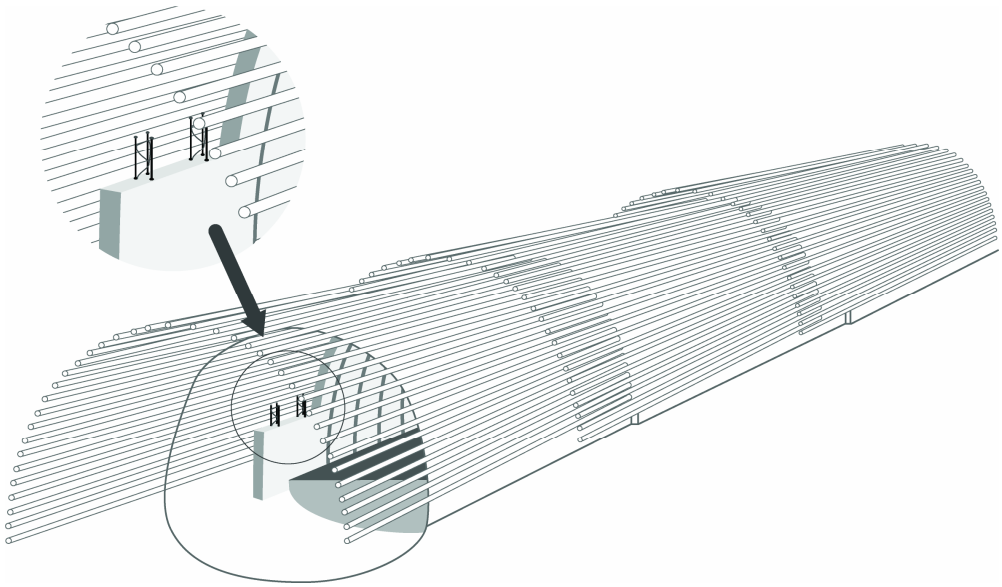

Fig. 3. Schematic of platform tunnel support.

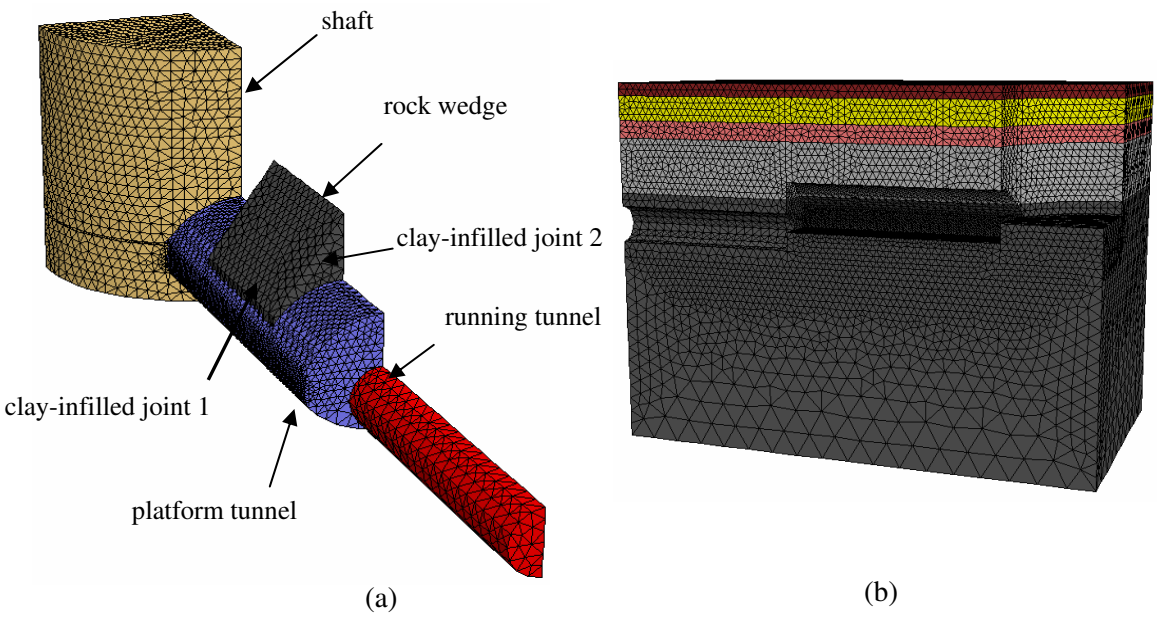

Fig. 4. Numerical model corresponding to one quarter of geometry. (a) Model components (b) End of bench excavation showing geotechnical units according to Table 2 (after Indraratna *et al.* 2009b).

Geological conditions at the Pinheiros Station site are marked by high levels of heterogeneity and anisotropy mainly due to prominent joint planes. The thicknesses of the different material layers (soils, weathered rock and fresh rock) vary significantly along the tunnel alignment increasing the difficulty

of establishing the contacts between materials (i.e. soils and rocks, weathered and fresh rock etc.) accurately along the entire tunnel. In addition, the station is located in an area known as the Caucaia Shear Zone, resulting in a highly fractured medium. The main joint sets are presented in Table 1. The main observed lithologies were biotite gneiss, granite gneiss and isolated pegmatite dykes. According to the Bieniawski classification (1989), the following rock mass classes were observed: II, III, IV (partially corresponding to saprolite) and V (partially corresponding to residual soils).

To take into account of the jointed medium, the rock mass classes II, III and IV were assumed to follow the Hoek-Brown failure criterion with elastic-perfectly-plastic behaviour. The elastic properties and strength parameters were estimated from the intact rock parameters adopting a value of the Geological Strength Index – GSI = 30, based on the geological structures and joint conditions (Fig. 5). It is assumed that this low value of GSI already takes into account the variability of the different material thicknesses, hence, a constant thicknesses for all layers were adopted as presented in Table 2 together with the relevant model parameters.

Table 1. Families of discontinuities (modified from IPT, 2008)

Joint set	Mean dip angle (°)	Mean dip direction (°)	Spacing (m)
F1	88	347	0.33
F2	89	73	0.38
F3	35	355	0.18
F4	40	161	0.27

Table 2. Geomechanical model parameters (after Indraratna *et al*. 2009b)

Layer	Elevation range (m)	E_i (MPA)	E_m (MPA)	ν	Mohr-Coulomb		Hoek-Brown				
					ϕ'	c' (kPa)	m_i	m_b	σ_{ci} (MPa)	a	s
Fill	724-721	8	-	0.30	24	1	-	-	-	-	-
Alluvium	721-716	15	-	0.30	28	5	-	-	-	-	-
Residual soil/Saprolite	716-712	100	-	0.30	28	15	-	-	-	-	-
Rock mass class IV	712-700	6380	519	0.25	-	-	16.42	1.35	5.8	0.52	4.2e-3
Rock mass class III	700-685	13000	1058	0.25	-	-	27.75	2.28	54.6	0.52	4.2e-3
Rock mass class II	685 -	27200	2200	0.25	-	-	32.6	2.68	60.0	0.52	4.2e-3

Due to the reduced confining or minor principal stress, σ_3, around the opening, the elements in that region were assigned a brittle behaviour to better simulate the failure of the top arch footings. The cohesion and tensile components of the strength are set to zero at the onset of yielding and the friction component is assumed half of its original value corresponding to a similar residual friction angle to that of the main joint sets ($\phi_r \approx 28°$).

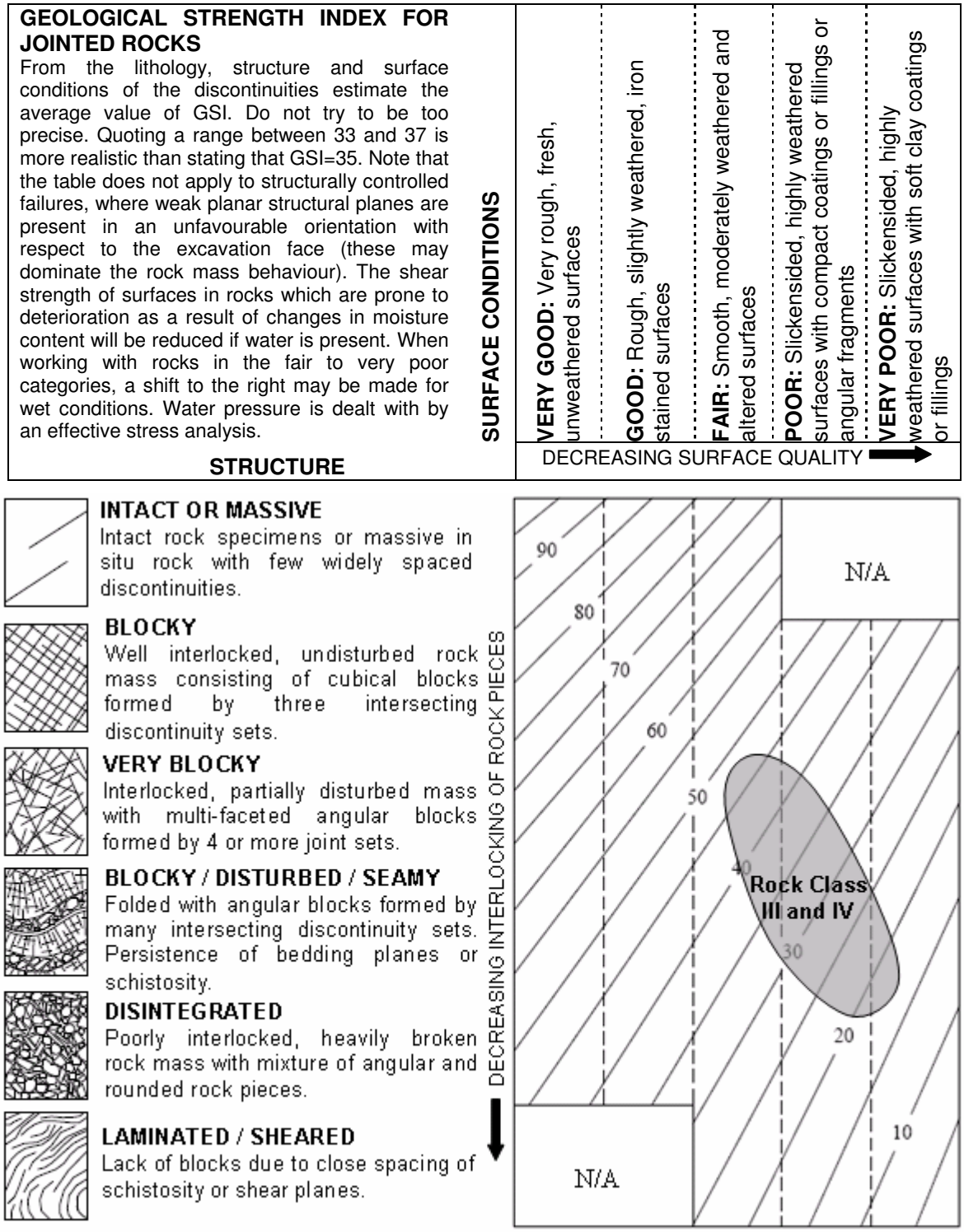

Fig. 5. Geological strength index for jointed rock masses (modified from Marinos and Hoek, 2000).

The in-situ stress ratio k_o was assumed equal to 1.0 before any excavation. This value of k_o was previously observed in similar excavations in the nearby area. No pore pressure measurements were

available, and despite the water table being above the roof of the tunnel, it was assumed that efficient drainage would occur through the fracture network during all stages of tunnelling.

The properties of the shotcrete lining were density ρ = 2500 kg/m^3, Young′s Modulus E = 30 GPa, compressive strength σ_c = 35 MPa and tensile strength σ_t = 3 MPa. The thicknesses of the shotcrete were t = 0.35 m and t = 0.15 m for the top arch and bench walls, respectively. Saiang *et al*. (2005) concluded that the interaction of the shotcrete lining and the country rock, thus the support effectiveness, is largely dependent on the behaviour of its interface. They also noted that the normal load applied to tunnel linings rarely exceeds 0.2 to 0.5 MPa, and under such a condition the shear strength is determined by the bond strength of cemented shotcrete-rock interfaces. As a result, shotcrete-rock interfaces also show a brittle behaviour. In light of this, the shotcrete-rock interface was discretised assigning a friction angle of ϕ_{cshot} = 50° and a cohesion of c_{cshot} = 250 kPa, which are similar to the equivalent friction angle and cohesion of the parent rock mass. At the onset of interface yielding, the cohesion is set to zero (i.e. c_{crshot} = 0). The lattice girder and forepole properties were, respectively: Young′s Modulus E_{lg} = 210 GPa and E_{fp} = 210 GPa, area A_{lg} = 15.64 x 10^{-4} m^2 and A_{fp} = 11.0 x 10^{-4} m^2, second moment of area I_{lg} = 752 x 10^{-8} m^4 and I_{fp} =6.37 x10^{-7} m^4 and plastic moment M_{lg} = 46.76 kN.m. and M_{fp} = 2.78 kN.m.

2.1 Clay-infilled discontinuities

As noted earlier, clay-infilled joints were observed during excavation which had not been taken into account in the design. Rock joints that are filled with soft sediments are likely to be the weakest planes in a rock mass, having a dominant influence on its overall shear behaviour. In this case, the joint material model adopted for the discontinuities should be able to describe important mechanisms such as asperity sliding and shearing, post-peak behaviour, asperity deformation, and the effect of the soft infilling.

Apart from the properties of the constituent materials, the infill thickness is perhaps the most important parameter controlling the strength of the joint. In non-planar joints, as the thickness of the infill to asperity amplitude ratio (*t/a*) increases, the overall shear strength of the joint decreases. Once a critical *t/a* ratio is attained, the joint walls no longer affect the overall behaviour and the joint shear strength may be represented by that of the infill alone.

Indraratna *et al.* (2009b) stated that, although not always clearly identified in laboratory results, three shearing phases can be assumed for infill thicknesses smaller than the critical value. The first phase is controlled mainly by the strength of the infill material. The role of the rock is to set the boundary limits for the soil failure surfaces which are defined by the geometry or roughness of the joint. During the second phase, as shearing proceeds, the infill above the sliding surface has to be “squeezed out” of its position between the advancing asperities to fill the space generated on the unloaded side of the

joint. After some displacement has occurred, the two rock surfaces will eventually come into contact and the strength of the joint will increase. From then on, the shear behaviour will be governed by the shape of the asperities and the strength of the rock, marking the beginning of the third phase. Depending on the level of applied normal stress, dilation may occur caused by sliding of one block over the other and be followed by the breakage of asperities as normally expected in unfilled joints.

Based on the above shearing mechanism Indraratna *et al.* (2009a) proposed the soil-infilled joint model which was further modified by Oliveira and Indraratna (2009b). Their model is based on a homogenised Coulombic slip model in which the effect of infill squeezing and asperity interference during shearing is accounted for. The current version of the soil-infilled joint model is given by:

$$\tau = \sigma_n \left(\left[\frac{\tan(\phi_b) + \tan(i_d)}{1 - \tan(\phi_b)\tan(i)} \right] \times (1-\eta) + \tan(\phi_r) \times \eta \right) \tag{1a}$$

where,

$$\eta = \exp\left(- \frac{u_s \times JRC}{100 \times c_1 \times a \times (t/a)} \right) \tag{1b}$$

$$i_d = (i_o - i)\exp\left(- \frac{(u_s - u_{peak})^2 \times JRC}{100 \times (c_2 \times a)^2} \right) + i \tag{1c}$$

$$i = \tan^{-1}\left(\frac{\partial u_n}{\partial u_s} \right) \tag{1d}$$

$$u_n = \frac{a_o}{2} + \sum_{n=1}^{N_h} L_f \left[a_n \cos\left(\frac{2\pi \times n \times u_s}{T} \right) + b_n \sin\left(\frac{2\pi \times n \times u_s}{T} \right) \right] \tag{1e}$$

In the above τ is the shear stress, σ_n is the normal stress, σ_{no} is the initial normal stress, ϕ_b is the basic friction angle of the rock joint, ϕ_r is a residual friction angle usually taken as the infill friction angle, i is the dilation angle at a given shear displacement, u_s, i_o is the initial asperity angle, u_n is the normal displacement, u_s is the accumulated shear displacement, u_{peak} is the shear displacement at peak stress ratio(τ/σ_n), η is the squeezing factor, c_1 and c_2 are empirical constants which control the rate of infill squeezing and asperity degradation respectively, a is the asperity amplitude, a_0, a_n and b_n are Fourier series coefficients, T is the Fourier period, N_h is number of harmonics, L_f the Lanczos sigma factor, *JRC* is the joint roughness coefficient and *t/a* the infill thickness to asperity amplitude ratio. It is of interest to note that in the case of *t/a*=0, *a*=0 or c_1=0 the user must enter a small number, say 10^{-5}, to avoid division by zero.

In this model, the proposed method for modelling dilation is by means of a Fourier series (Eq. 1e) which is fitted to the normal displacements obtained experimentally. Hence, the dilation angle, which changes with shear displacement, is exactly that observed during the shear tests, as represented by Eq. (1d). The constants a_n and b_n are found by performing conventional harmonic analysis of Fourier Series. The Fourier constants vary with the initial normal stress applied to the joint, σ_{no}, and boundary conditions. Therefore, these constants must be found for the range of expected σ_{no}. Intermediate values of σ_{no} are then interpolated in a piecewise linear fashion. If the joints are subjected to a confined condition in the field, as around underground excavations, the laboratory tests should also simulate such condition which may be accomplished by conducting the tests under constant normal stiffness (CNS) rather than under a constant normal loading condition (CNL). Further details on the application of Fourier Series for modelling joint dilation, the determination of Fourier coefficients and direct shear test under CNS condition are presented by Indraratna *et al.* (1999) and Oliveira and Indraratna (2009a). It is important to remark that there are numerous uncertainties in analysing and predicting dilation in practice and, as with others methods of modelling dilation, the Fourier series should be carefully considered.

For infill thicknesses smaller than the critical value, a hardening behaviour is often observed in laboratory results which is caused by the increase in joint roughness influence with shear displacement. This mechanism is captured by the soil-infilled joint model due to the concepts of infill squeezing and asperity interference. Similar behaviour was also reported by de Toledo and de Freitas (1993). This hardening/softening behaviour is not readily described by conventional joint models such as the Coulomb slip and Barton-Bandis models. As a result, an overestimation of the shear strength would be observed in the first and second phase of the shear-strain curve, thus, under-predicting the joint shear displacements.

In order to investigate the behaviour of the rock wedge under a condition of pronounced infill squeezing and asperity interference, the clay-infilled joint reported by Indraratna and Jayanathan (2005) presented in Fig. 6 was assumed to be representative of the existing joints (Fig. 4). Possible scale effects were disregarded and the thickness of the infill was assumed constant along the joints. Due to the difference in predicting the mobilisation of the shear strength, both Coulomb slip joint and soil-infilled joint models were adopted and the effect on wedge stability evaluated. The implementation of the soil-infilled joint model in FLAC3D is discussed by Indraratna *et al.* (2009b).

Fig. 6 shows the good agreement of the soil-infilled joint model for both shear-strain and normal displacement data whereas the Coulomb slip model overestimates the shear strength for axial strain lower than the peak as discussed earlier. The parameters for the soil-infilled joint model are presented in Table 3. For the Coulomb slip model, the same shear stiffness and normal stiffness are used with a friction angle ϕ_{peak}= 41°.

Table 3. Soil-infilled joint model parameters for triaxial test on clay-infilled joints (after Indraratna *et al*. 2009b).

σ_3	t/a	ϕ_b	ϕ_r	i_o	JRC	a (mm)	c_1	c_2	u_{peak} (mm)	k_n (kPa/mm)	k_s (kPa/mm)
200	0.5	37º	24º	18	18	2.00	0.85	0.15	4.1	1.5e7	3.0e5
500	0.5	37º	24º	18	18	2.00	0.85	0.15	3.5	1.5e7	1.5e6

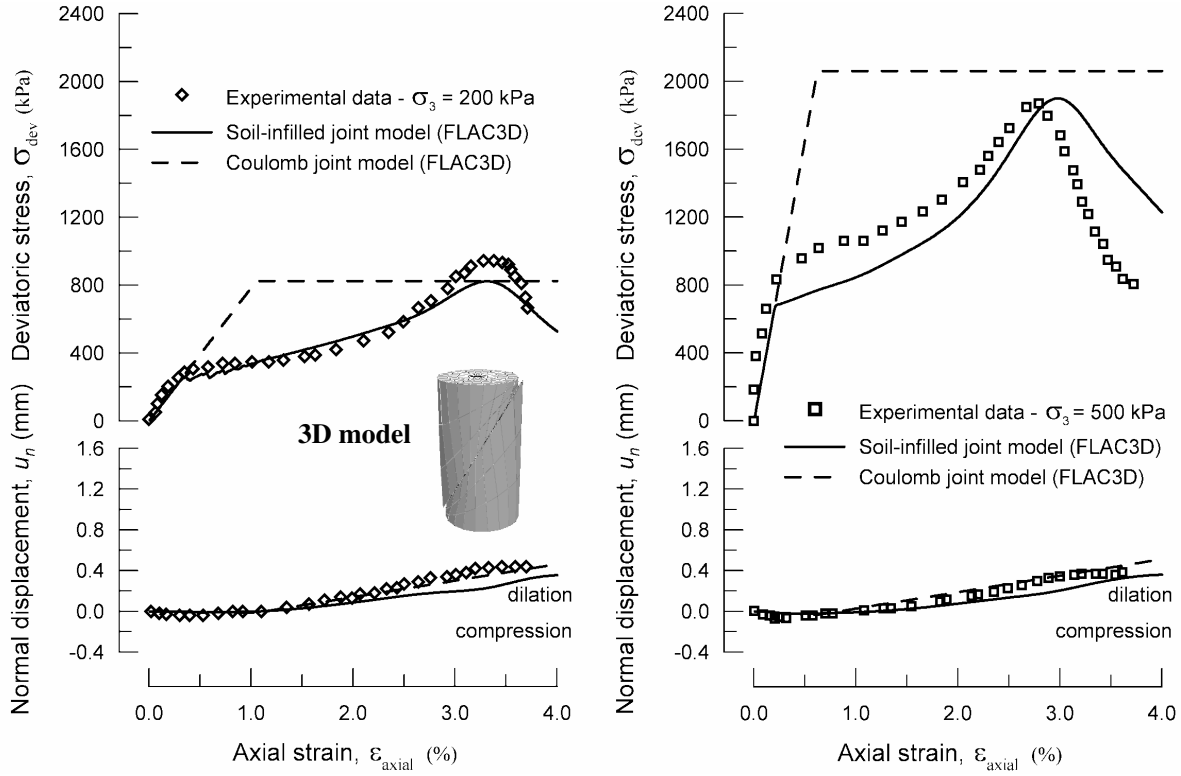

Fig. 6. Prediction of joint models for triaxial tests on clay-infilled joints with *t/a* = 0.5 (after Indraratna *et al*. 2009b).

3 MODEL RESULTS

It is apparent from Fig. 7 that the model describes the tunnel behaviour during excavation with acceptable agreement. The displacements predicted with the soil-infilled joint model are in agreement with the higher displacements observed in the field and, as expected, are about 10% higher than those predicted by the Coulomb slip joint model.

Despite the good agreement of the predicted displacements with the instrumentation data, only the data shown in Fig. 7 do not clearly indicate collapse. Therefore, it is important to verify the structural performance of the tunnel support for the observed level of deformation. Potential failure of the support system can be noted when plotting the structural capacity diagram of the top heading shotcrete lining underneath the rock wedge (Fig. 8). The shaded area represents the maximum loading combination (axial force vs bending moment), and its limit (solid line) is the envelope for the onset of

cracking (F_{os}= 1). The construction and interpretation of the capacity diagrams in Fig. 8 are based on the solutions presented by Hoek *et al*. (2008) and Carranza-Torres and Diederichs (2009). Although the soil-infilled joint model predicts slightly higher induced moments and axial loads as the result of the predicted larger displacements, both joint models indicate the potential failure of the support.

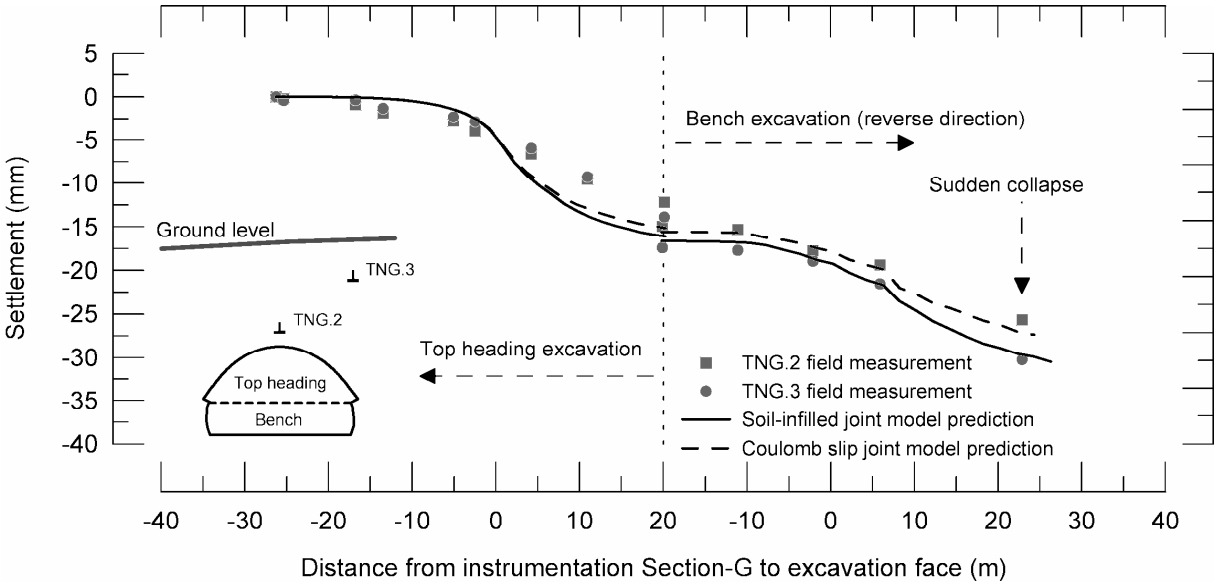

Fig. 7. Settlement predictions with tunnel advance at instrumentation section G, 27 m away from shaft (after Indraratna *et al*. 2009b).

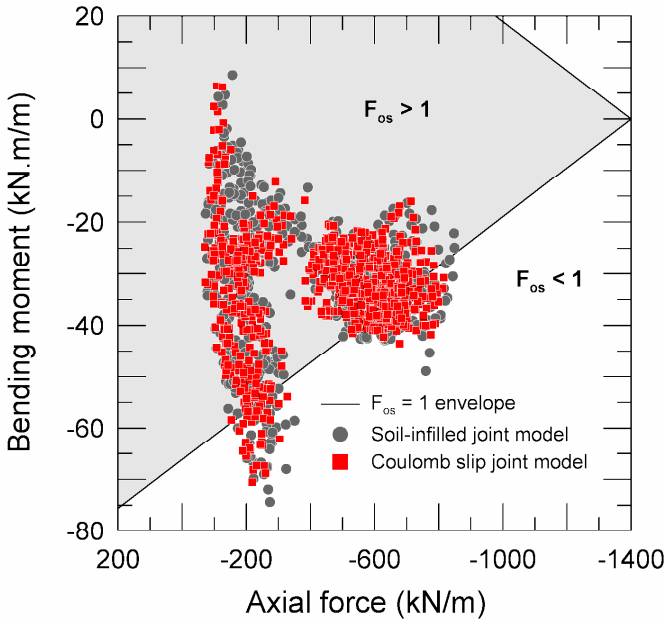

Fig. 8. Support capacity diagram of top heading shotcrete lining after bench excavation (after Indraratna *et al*. 2009b).

It is important to remark that in this analysis only the joints controlling the roof wedge have been fully discretised and the remaining joint sets have been accounted for through an equivalent continuunm

material model, i.e. the Hoek-Brown model. Therefore, the difference between the two joint models in the overall tunnel behaviour is less pronounced than that if a 3D discontinuous model had been employed discretising all joint sets. However, the effect of the different joint models is much more pronounced in the behaviour of rock wedge alone. As shown in Fig. 9, the Coulomb slip model predicts the mobilisation of the shear strength of joint 1 in Fig. 4 at significantly lower displacements (approximately 150% less) than does the soil-infilled joint model. The higher the displacements, the smaller will be the normal stress acting on the joint due to the stress relaxation implied in the wedge stability. Consequently, the soil-infilled joint model indicates a more obvious detachment of the wedge from the tunnel roof, which justifies the differences observed in Figs 7 and 8.

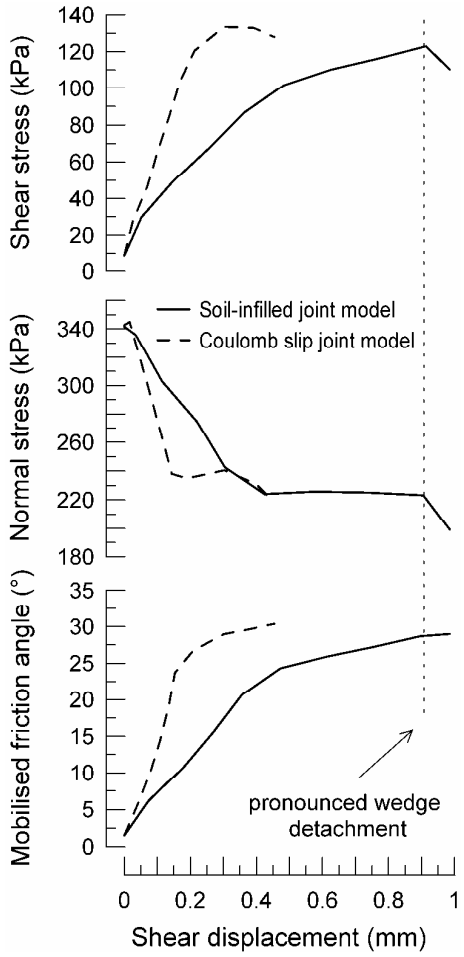

Fig. 9. Prediction of wedge behaviour and mobilisation of the shear strength of joint 1 (after Indraratna *et al.* 2009b).

The collapse kinematics modelled in this study can be summarised according to the following stages: (a) before excavation; (b) excavation of the top heading causing low to moderate wedge displacements; (c) excavation of the cavern bench causing further wedge displacement (i.e. failure of the rock mass underneath the footings due to the removal of confinement

causes pronounced wedge detachment); and (d) the pronounced displacement of the wedge overloads the support system which progressively fails. Fig. 10 depicts the stages of the collapse observed in the current model which is in agreement with the sequence of the failure mechanism presented by IPT (2008) and Barros *et al*. (2008).

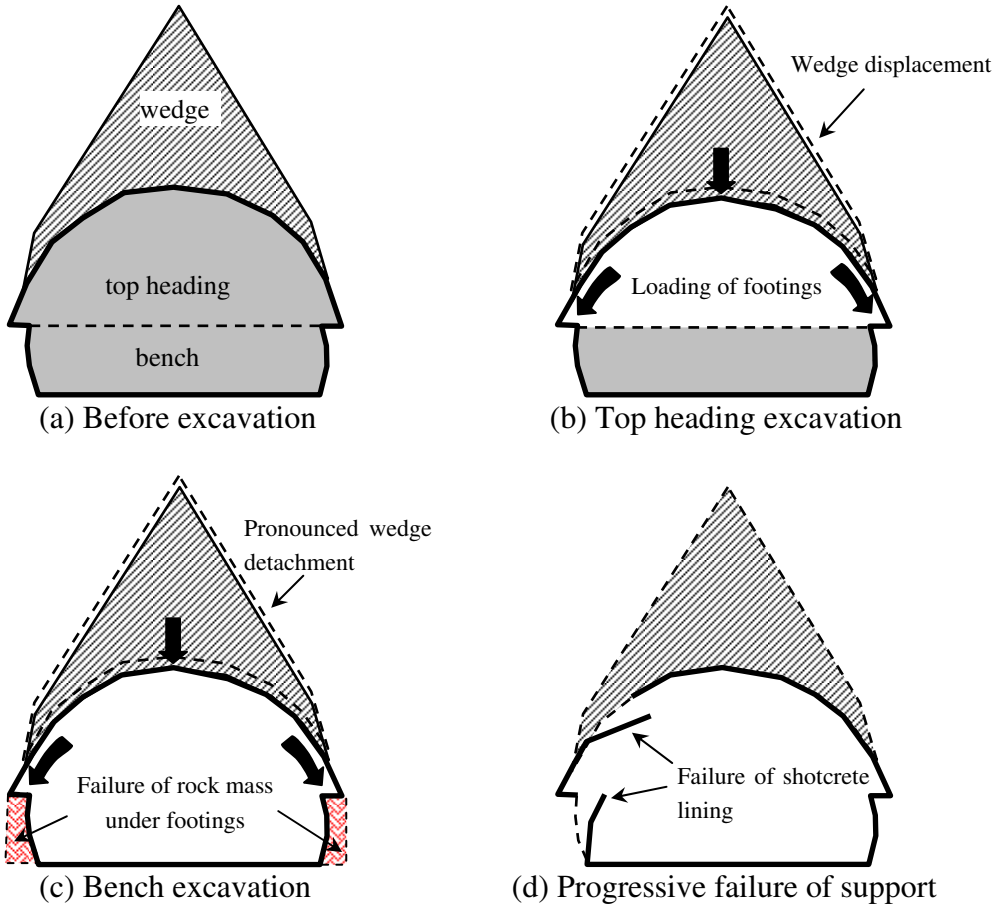

Fig. 10. Kinematics of cavern collapse (after Indraratna *et al*. 2009b).

4 CONCLUSIONS

A back-analysis based on the Pinheiros Station collapse was presented in order to investigate a possible failure mechanism. The influence of a large rock wedge in the cavern roof and the failure of the rock mass underneath the arch footings were simulated. Moreover, the effects of clay-infilled rock joints with pronounced roughness and infill squeezing influence were also considered.

Besides the obvious effect of reducing the shear strength of rock joints, the presence of a soft sediment infill may impose strain hardening and/or strain softening mechanisms which are often associated with an increase in joint roughness influence and infill squeezing with

displacement. This hardening/softening behaviour is not described by joint models such as the Coulomb slip and Barton-Bandis, and the use of these models may yield an overestimation of the mobilised shear strength and an underestimation the joint shear displacements.

The numerical model, which represented the observed collapse with acceptable agreement, clearly demonstrates that the delayed mobilisation of the shear strength generates not only larger displacements of the rock wedge, but also causes larger overall tunnel deformation and increased support loads.

ACKNOWLEDGEMENTS

The Author is grateful for the supervision of Prof. Buddhima Indraratna during his PhD studies. The collaboration of Prof. E.T. (Ted) Brown is also appreciated. It is also important to acknowledge the essential collaboration of Prof. André Assis, who was one of the leading consultants for the IPT during the investigation of the Pinheiros collapse.

REFERENCES

Barros JM, Iyomasa W, Azevedo AA, Eisenstein Z, Assis, AP (2008). Lessons from Brazil: Pinheiros examined. Tunnels & Tunnelling International, November issue.

Barton N (2008). A summary of the main factors that caused the uniquely sudden collapse at Pinheiros. Seminar at the Institution of Engineers, Sao Paulo, Brazil (unpublished note).

Bieniawski ZT (1989). Engineering rock mass classification. New York: Wiley.

Carranza-Torres C, Diederichs M (2009). Mechanical analysis of circular liners with particular reference to composite supports. For example, liners consisting of shotcrete and steel sets. *Tunnelling and Underground Space Technology*, 24(5), pp 506-532.

de Toledo PEC, de Freitas MH (1993). Laboratory testing and parameters controlling the shear strength of filled rock joints. *Géotechnique*, 43(1), pp 1-19.

Hoek E, Carranza-Torres C, Diederichs MS, Corkum, B (2008). Kersten Lecture. Integration of geotechnical and structural design in tunneling. In: Proceedings of the University of Minnesota 56th annual geotechnical engineering conference, Minneapolis, 29 February.

Indraratna B, Haque A, Aziz N (1999). Shear behaviour of idealized infilled joints under constant normal stiffness. *Géotechnique*, 49(3), pp 331-355.

Indraratna B, Jayanathan M (2005). Measurement of pore water pressure of clay-filled rock joints during triaxial shearing. *Géotechnique*, 55(10), pp759-764.

Indraratna B, Oliveira DAF, Brown ET (2009a). A shear-displacement criterion for soil-infilled rock discontinuities. *Géotechnique* (accepted April 2009).

Indraratna B, Oliveira DAF, Brown ET, Assis AP (2009b). Effect of soil-infilled joints on the stability of rock wedges formed in a tunnel roof. *Int. J. of Rock. Mech. and Mining Sciences* (under review).

IPT (2008). Technical Report: Investigation and Analysis of the Pinheiros Station collapse. Institute for Technological Research - IPT, Sao Paulo, Brazil (in Portuguese).

Maffei C, Nieble C M, Sadowski G R, Takahashi J, de Mello L G (2008). Diagnostic of the Pinheiros Station collapse. Seminar at the Institution of Engineers, Sao Paulo, Brazil (unpublished note, in Portuguese).

Marinos, P and Hoek, E. (2000). GSI – A geologically friendly tool for rock mass strength estimation. *Proc. GeoEng2000 Conference*, Melbourne, pp. 1422-1442

Oliveira DAF, Indraratna B (2009a). Numerical modelling of soil-infilled rock discontinuities. *Australian Geomechanics*, 44(1), pp 49-58.

Oliveira DAF, Indraratna B (2009b). A comparison between models of rock discontinuity strength and deformation. *J Geotech Geoenvir Engng ASCE* (under review).

Saiang D, Malmgren L, Nordlund E (2005). Laboratory tests on shotcrete-rock joints in direct shear, tension and compression. *Rock Mech. Rock Engng*, 38(4), pp 275-297.